Available online at www.sciencedirect.com

ScienceDirect

European Journal of Mechanics A/Solids 25 (2006) 695–706

Bleustein–Gulyaev waves in some functionally graded materials

Bernard Collet, Michel Destrade *, Gérard A. Maugin

Laboratoire de Modélisation en Mécanique, CNRS (UMR7607), Université Pierre et Marie Curie, case 162, 4, place Jussieu, 75252 Paris cedex 05, France

Received 25 July 2005; accepted 26 January 2006

Available online 28 February 2006

Abstract

Functionally Graded Materials are inhomogeneous elastic bodies whose properties vary continuously with space. Hence consider a half-space ($x_2 > 0$) occupied by a special Functionally Graded Material made of an hexagonal (6 mm) piezoelectric crystal for which the elastic stiffness c_{44}, the piezoelectric constant e_{15}, the dielectric constant ϵ_{11}, and the mass density, all vary proportionally to the same "inhomogeneity function" $f(x_2)$, say. Then consider the problem of a piezoacoustic shear-horizontal surface wave which leaves the interface ($x_2 = 0$) free of mechanical tractions and vanishes as x_2 goes to infinity (the Bleustein–Gulyaev wave). It turns out that for some choices of the function f, this problem can be solved exactly for the usual boundary conditions, such as metalized surface or free surface. Several such functions $f(x_2)$ are derived here, such as $\exp(\pm 2\beta x_2)$ (β is a constant) which is often encountered in geophysics, or other functions which are periodic or which vanish as x_2 tends to infinity; one final example presents the advantage of describing a layered half-space which becomes asymptotically homogeneous away from the interface. Special attention is given to the influence of the different inhomogeneity functions upon the characteristics of the Bleustein–Gulyaev wave (speed, dispersion, attenuation factors, depth profiles, electromechanical coupling factor, etc.)

Keywords: Bleustein–Gulyaev wave; Functionally graded materials; Exact solutions

1. Introduction

The wireless communication industry (mobile phones, global positioning systems, pagers, label identification tags, etc.) fuels most of the current mass production of Surface Acoustic Wave devices (more than 1 billion units/year) where SAW-based interdigital transducers are used as high-frequency filters. In the race for miniaturization, devices based on Bleustein–Gulyaev waves (pure shear-horizontal mode) technology have proved more apt for downsizing than those based on Rayleigh waves (two- or three-partial modes) technology, according to Kadota et al. (2001).

Can the so-called "Functionally Graded Materials", whose properties vary continuously in space, be used to improve the efficiency of Bleustein–Gulyaev waves? For a 6 mm piezoelectric *homogeneous substrate*, the classic solution of Bleustein (1968) and Gulyaev (1969) is quite simple to derive; for a *functionally graded substrate*, the corresponding wave solution is in general impossible to determine analytically. In order to make progress, and with a view to use the eventual results as benchmarks for more complicated simulations, this paper strikes a compro-

* Corresponding author. Tel.: +33 1 4427 7166; fax: +33 1 4727 5259.
E-mail address: destrade@lmm.jussieu.fr (M. Destrade).

0997-7538/$ – see front matter
doi:10.1016/j.euromechsol.2006.01.007

mise between these two extreme situations, and aims at finding in a simple way certain types of functionally graded substrates for which analytical Bleustein–Gulyaev type of solutions are easily derived. Such a task can be achieved by making the assumption that for the functionally graded material, the elastic stiffness c_{44}, the piezoelectric constant e_{15}, the dielectric constant ϵ_{11}, *and* the mass density ρ, all vary in the same proportion with a single space variable. This assumption is often encountered in the literature, see for example the recent articles (Jin et al., 2003; Kwon and Lee, 2003; Wang, 2003; Chen et al., 2004; Kwon, 2004; Ma et al., 2004; Chen and Liu, 2005a, 2005b; Guo et al., 2005a, 2005b; Ma et al., 2005a, 2005b; Pan and Han, 2005; Sladek et al., 2005; Sun et al., 2005; Feng and Su, 2006). It is a strong assumption, which can be envisaged to hold for c_{44}, e_{15}, ϵ_{11} in certain contexts (pre-stressed laminae (Cohen and Wang, 1992), elastic bodies subjected to a thermal gradient (Saccomandi, 1999), continuously twisted structurally chiral media (Lakhtakia, 1994), etc.), but is unlikely to hold for ρ as well. However, this assumption proves crucial for the derivation of analytical results in terms of "simple" functions such as the polynomial, sinusoidal, and hyperbolic functions. Previous studies have indeed shown that if ρ behaves differently from the other material quantities, then analytical solutions of the shear-horizontal wave problem involve special functions such as Bessel functions (Wilson, 1942; Bhattacharya, 1970; Maugin, 1983), Hankel functions (Deresiewicz, 1962), Whittaker functions (Deresiewicz, 1962; Bhattacharya, 1970), hypergeometric functions (Bhattacharya, 1970; Viktorov, 1979; Maugin, 1983), etc. (see the review by Maugin (1983) for some pointers to the wide literature on the subject); otherwise, numerical and approximate methods are necessary to solve the problem, such as those based on Laguerre series (Gubernatis and Maradudin, 1987), on a combination of Fast Fourier Transforms and modal analysis (Liu and Tani, 1994), on Legendre polynomials (Lefebvre et al., 2001), on the WKB approximation (Liu and Wang, 2005), etc.

In short, some generality is lost by taking ρ to behave in the same manner as the other quantities, but some simplicity and insights are gained, because the resulting exact solutions may serve as benchmarks for more realistic situations, where for instance a perturbation boundary element method can be used (Azis and Clements, 2001). The governing equations derived in the course of this paper can also be specialized to the consideration of anti-plane deformations in the context of piezo-elastostatic problems, where the density plays no role and its eventual spatial variations need not be specified.

The paper begins the analysis in Section 2 with the derivation of the equations governing the propagation of a Shear–Horizontal wave in the type of Functionally Graded Material just discussed. In Section 3, a change of unknown functions leads to the decoupling of the four first-order governing equations into two separate pairs of second-order differential equations. For certain choices of inhomogeneity, the differential equations have constant coefficients and the consequences of such choices on the propagation of Bleustein–Gulyaev waves are fully analyzed and are illustrated numerically by two examples: one where the inhomogeneity is a decreasing exponential function, the other where it is an inverse quadratic function. The last two sections show that other inhomogeneity functions leading to explicit results can be generated, not necessarily by seeking differential equations with constant coefficients. Section 4 focuses on an inhomogeneity function for which the material parameters vary smoothly from a value at the interface to an asymptotic value at infinite distance from the interface. Section 5 presents one method, presumably among many others, to generate an infinity of inhomogeneity functions leading to exact Bleustein–Gulyaev solutions.

2. A certain type of functionally graded materials

The Bleustein–Gulyaev wave is a shear horizontal wave, traveling over the surface of a semi-infinite piezoelectric solid for which the sagittal plane is normal to a binary axis of symmetry. Now consider a half-space $x_2 \geqslant 0$ (say), made of a piezoelectric crystal with 6 mm symmetry (see e.g. Royer and Dieulesaint, 2000) and with continuously varying properties in the x_2-direction. Specifically, the elastic stiffness c_{44}, the piezoelectric constant e_{15}, the dielectric constant ϵ_{11}, and the mass density ρ, all vary in the same proportion with depth x_2:

$$\left\{c_{44}(x_2), e_{15}(x_2), \epsilon_{11}(x_2), \rho(x_2)\right\} = \left\{c_{44}^{\circ}, e_{15}^{\circ}, \epsilon_{11}^{\circ}, \rho^{\circ}\right\} f(x_2), \tag{2.1}$$

where c_{44}°, e_{15}°, ϵ_{11}°, ρ° are constants, and f is a yet unspecified function of x_2, henceforward called the *inhomogeneity function*. Without loss of generality, f is normalized as $f(0) = 1$.

Now take two orthogonal directions x_1, x_3 in the plane $x_2 = 0$ such that the symmetry axis is along x_3 and consider the propagation of a Bleustein–Gulyaev wave, traveling with speed v and wave number k in the x_1-direction. The associated quantities of interest are: the mechanical displacement component u_3, the electric potential ϕ, the mechanical traction components σ_{13}, σ_{23}, and the electric displacement components D_1, D_2. They are taken in the form

$$\{u_3, \phi, \sigma_{j3}, D_j\}(x_1, x_2, t) = \{U_3(x_2), \varphi(x_2), \mathrm{i}t_{j3}(x_2), \mathrm{i}d_j(x_2)\}\, \mathrm{e}^{\mathrm{i}k(x_1 - vt)}, \tag{2.2}$$

where U_3, φ, t_{j3}, d_j $(j = 1, 2)$ are unknown functions of x_2 alone, to be determined from the piezoacoustic equations and from the boundary conditions.

In the present context, the classical equations of piezoacoustics written in the quasi-electrostatic approximation,

$$\frac{\partial \sigma_{ij}}{\partial x_j} = \rho \frac{\partial^2 u_i}{\partial t^2}, \qquad \frac{\partial D_j}{\partial x_j} = 0, \tag{2.3}$$

decouple entirely the anti-plane stress and strain from their in-plane counterparts. The anti-plane equations can be written as a first-order differential system,

$$\begin{bmatrix} \boldsymbol{u}' \\ \boldsymbol{v}' \end{bmatrix} = \mathrm{i} \begin{bmatrix} \mathbf{0} & \frac{1}{f(x_2)} \boldsymbol{N}_2 \\ k^2 f(x_2) \boldsymbol{K} & \mathbf{0} \end{bmatrix} \begin{bmatrix} \boldsymbol{u} \\ \boldsymbol{v} \end{bmatrix}, \quad \text{where } \boldsymbol{u} := \begin{bmatrix} U_3 \\ \varphi \end{bmatrix}, \ \boldsymbol{v} := \begin{bmatrix} t_{23} \\ d_2 \end{bmatrix}, \tag{2.4}$$

and $\boldsymbol{N}_2$, $\boldsymbol{K}$ are the following constant symmetric matrices,

$$\boldsymbol{N}_2 := \frac{1}{c^\circ_{44}\epsilon^\circ_{11} + e^{\circ 2}_{15}} \begin{bmatrix} \epsilon^\circ_{11} & e^\circ_{15} \\ e^\circ_{15} & -c^\circ_{44} \end{bmatrix}, \qquad \boldsymbol{K} := \begin{bmatrix} \rho^\circ v^2 - c^\circ_{44} & -e^\circ_{15} \\ -e^\circ_{15} & \epsilon^\circ_{11} \end{bmatrix}. \tag{2.5}$$

3. Some simple inhomogeneity functions

In this section, attention is restricted to some inhomogeneity functions for which the piezoacoustic equations turn into linear ordinary differential equations with *constant* coefficients.

3.1. Further decoupling of the piezoacoustic equations

With the new vector functions $\hat{\boldsymbol{u}}$ and $\hat{\boldsymbol{v}}$, defined as

$$\hat{\boldsymbol{u}}(x_2) := \sqrt{f(x_2)}\, \boldsymbol{u}(x_2), \qquad \hat{\boldsymbol{v}}(x_2) := \boldsymbol{v}(x_2)/\sqrt{f(x_2)}, \tag{3.1}$$

the system (2.4) becomes

$$\begin{bmatrix} \hat{\boldsymbol{u}}' \\ \hat{\boldsymbol{v}}' \end{bmatrix} = \begin{bmatrix} \frac{p}{2}\mathbf{1} & \mathrm{i}\boldsymbol{N}_2 \\ \mathrm{i}k^2\boldsymbol{K} & -\frac{p}{2}\mathbf{1} \end{bmatrix} \begin{bmatrix} \hat{\boldsymbol{u}} \\ \hat{\boldsymbol{v}} \end{bmatrix}, \quad \text{where } p := \frac{f'}{f}. \tag{3.2}$$

Now, by differentiation and substitution, an entirely decoupled second-order system emerges:

$$\begin{bmatrix} \hat{\boldsymbol{u}}'' \\ \hat{\boldsymbol{v}}'' \end{bmatrix} = - \begin{bmatrix} k^2 \boldsymbol{N_2 K} - (\frac{p^2}{4} + \frac{p'}{2})\mathbf{1} & \mathbf{0} \\ \mathbf{0} & k^2 \boldsymbol{K N_2} - (\frac{p^2}{4} - \frac{p'}{2})\mathbf{1} \end{bmatrix} \begin{bmatrix} \hat{\boldsymbol{u}} \\ \hat{\boldsymbol{v}} \end{bmatrix}, \tag{3.3}$$

and two simple ways of finding exact solutions for shear-horizontal wave propagation appear naturally.

- Either (i) solve

  $$\frac{p^2}{4} + \frac{p'}{2} = c_0, \tag{3.4}$$

  where c_0 is a constant. Then the solution $\hat{\boldsymbol{u}}$ to the second-order equation $(3.3)_1$ with (now) *constant* coefficients is easily found. Finally, $\boldsymbol{u}$ follows from $(3.1)_1$ and $\boldsymbol{v}$ from the inversion of $(2.4)_1$,
- Or (ii) solve

  $$\frac{p^2}{4} - \frac{p'}{2} = c_0, \tag{3.5}$$

  where c_0 is a constant. Then the solution $\hat{\boldsymbol{v}}$ to the second-order equation $(3.3)_2$ with (now) *constant* coefficients is easily found. Finally, $\boldsymbol{v}$ follows from $(3.1)_2$ and $\boldsymbol{u}$ from the inversion of $(2.4)_2$.

Table 1
Some simple inhomogeneity functions

	c_0	$p(x_2)$	$f(x_2)$
P0	β^2	$\pm 2\beta$	$\exp(\pm 2\beta x_2)$
P1	0	$2\beta/(\beta x_2+1)$	$(\beta x_2+1)^2$
P2	β^2	$2\beta \tanh(\beta x_2+\delta)$	$\dfrac{\cosh^2(\beta x_2+\delta)}{\cosh^2\delta}$
P3	β^2	$2\beta/\tanh(\beta x_2+\delta)$	$\dfrac{\sinh^2(\beta x_2+\delta)}{\sinh^2\delta}$
P4	$-\beta^2$	$-2\beta\tan(\beta x_2+\delta)$	$\dfrac{\cos^2(\beta x_2+\delta)}{\cos^2\delta}$
P5	$-\beta^2$	$2\beta/\tan(\beta x_2+\delta)$	$\dfrac{\sin^2(\beta x_2+\delta)}{\sin^2\delta}$
P6	0	$-2\beta/(\beta x_2+1)$	$\dfrac{1}{(\beta x_2+1)^2}$
P7	β^2	$-2\beta\tanh(\beta x_2+\delta)$	$\dfrac{\cosh^2\delta}{\cosh^2(\beta x_2+\delta)}$
P8	β^2	$-2\beta/\tanh(\beta x_2+\delta)$	$\dfrac{\sinh^2\delta}{\sinh^2(\beta x_2+\delta)}$
P9	$-\beta^2$	$2\beta\tan(\beta x_2+\delta)$	$\dfrac{\cos^2\delta}{\cos^2(\beta x_2+\delta)}$
P10	$-\beta^2$	$-2\beta/\tan(\beta x_2+\delta)$	$\dfrac{\sin^2\delta}{\sin^2(\beta x_2+\delta)}$

Of course the two possibilities (3.4) and (3.5) do not exhaust the classes of solutions. The last section of this article shows how infinitely more inhomogeneous profiles can be generated.

Clearly now, if p is solution to (3.4), then $-p$ is solution to (3.5); so that if f is solution to (3.4), then $1/f$ is solution to (3.5). The resolution of these two equations is straightforward, and the results are collected in Table 1: according as to whether c_0 is positive, negative, or equal to zero (second column), several functions $p(x_2)$ (third column) and $f(x_2)$ (fourth column) are found. The inhomogeneity profile P0 is common to the resolution of (3.4) and (3.5); profiles P1–P5 result from (3.4) and P6–P10 from (3.5). The quantities β (inverse of a length) and δ (non-dimensional) are arbitrary, so that the inhomogeneity functions $f(x_2)$ in P4 and P5 are essentially the same functions, and so are the inhomogeneity functions in P9 and P10.

Some of these inhomogeneity functions are often encountered in the geophysics literature, such as the exponential function P0 or the quadratic function P1. Dutta (1963) used P2 for Love waves; Erdogan and Ozturk (1992) and Hasanyan et al. (2003) derived P0–P5 in a different (purely elastic) context; P6–P10 appear to be new, presumably because the preferred second-order form of the equations of motion is usually $(3.3)_1$ rather than $(3.3)_2$ (see Destrade, 2001, for a discussion on this latter point).

The functions found present the advantages of mathematical simplicity and familiarity. Each of them however presents the inconvenience of describing a somewhat unrealistic inhomogeneity, because each either blows up or vanishes as $x_2 \to \infty$, or blows up or vanishes periodically. These problems can be overcome by considering that they occur sufficiently far away from the interface, and by focusing on the near-the-surface localization of the wave.

3.2. Exact solution

Here the emphasis is on the complete resolution for the Bleustein–Gulyaev wave in Case (i) (profiles P0–P5). In Case (ii), the resolution is very similar, and the corresponding results are summarized at the end of this subsection.

First, solve the decoupled, second-order, linear, with constant coefficients, differential equation $(3.3)_1$ for $\hat{\boldsymbol{u}}$:

$$\hat{\boldsymbol{u}}'' + \left(k^2 \boldsymbol{N_2 K} - c_0 \mathbf{1}\right)\hat{\boldsymbol{u}} = \mathbf{0}, \tag{3.6}$$

with a solution in exponential evanescent form,

$$\hat{\boldsymbol{u}}(x_2) = \mathrm{e}^{-kqx_2}\widehat{\boldsymbol{U}}^{\mathbf{0}}, \quad \Re(q) > 0, \tag{3.7}$$

where $\widehat{\boldsymbol{U}}^{\boldsymbol{0}}$ is constant and q is an attenuation factor. Then $\widehat{\boldsymbol{U}}^{\boldsymbol{0}}$ and q are solutions to

$$\left[k^2\boldsymbol{N_2K} - \left(c_0 - k^2q^2\right)\boldsymbol{1}\right]\widehat{\boldsymbol{U}}^{\boldsymbol{0}} = \boldsymbol{0}. \tag{3.8}$$

The associated determinantal equation is the *propagation condition*, here

$$\left[k^2\left(q^2 - 1 - \left(v/v_T^\circ\right)^2 - c_0\right)\right]\left[k^2\left(q^2 - 1\right) - c_0\right] = 0, \tag{3.9}$$

where v_T° is the speed of the bulk shear wave in the homogeneous ($f \equiv 1$) material, given by

$$\rho^\circ v_T^{\circ 2} = c_{44}^\circ + e_{15}^{\circ 2}/\epsilon_{11}^\circ. \tag{3.10}$$

The *attenuation factors* q_1, q_2 (say) with positive real part are

$$q_1 = \sqrt{1 + c_0/k^2 - \left(v/v_T^\circ\right)^2}, \qquad q_2 = \sqrt{1 + c_0/k^2}, \tag{3.11}$$

provided the speed belongs to the subsonic interval

$$0 < \left(v/v_T^\circ\right)^2 < 1 + c_0/k^2. \tag{3.12}$$

The smallest of these two quantities (q_1) is indicative of the *penetration depth*. Here, the inhomogeneity affects the penetration depth in the following manners: for the exponential profile P0 and for the hyperbolic profiles (P2, P3, P7, P8), the wave is more localized than in the homogeneous case ($f \equiv 1$); for the trigonometric profiles (P4, P5, P9, P10), the wave penetrates further into the substrate; for the polynomial profiles (P1, P6), the penetration depth is the *same* as in the homogeneous case. Note in passing that the inequality (3.12) puts an upper bound on the possible values of β for the trigonometric profiles P4, P5, P9, P10 (where $c_0 = -\beta^2$), namely: $\beta^2 < k^2$, which means that the wavelength of the wave must be smaller than the wavelength of those profiles. These remarks are however preliminary and concern the behavior of the functions $\hat{\boldsymbol{u}}$ and $\hat{\boldsymbol{v}}$ with depth. The behavior of the wave itself is dictated by the functions $\boldsymbol{u}$ and $\boldsymbol{v}$, see (3.1). In particular, inequality (3.12) ensures that $\hat{\boldsymbol{u}}(\infty) = \boldsymbol{0}$ but, because $\boldsymbol{u} = (1/\sqrt{f})\hat{\boldsymbol{u}}$, not necessarily that $\boldsymbol{u}(\infty) = \boldsymbol{0}$; this latter condition must be tested a posteriori against each different form of f.

Now the constant vectors $\widehat{\boldsymbol{U}}^{\boldsymbol{1}}$, $\widehat{\boldsymbol{U}}^{\boldsymbol{2}}$ (say) satisfying (3.8) when $q = q_1, q_2$, respectively, are easily computed and the general solution to (3.6) is constructed as: $\hat{\boldsymbol{u}}(x_2) = \gamma_1 \mathrm{e}^{-kq_1x_2}\widehat{\boldsymbol{U}}^{\boldsymbol{1}} + \gamma_2 \mathrm{e}^{-kq_2x_2}\widehat{\boldsymbol{U}}^{\boldsymbol{2}}$ where γ_1, γ_2 are constant scalars. Explicitly,

$$\hat{\boldsymbol{u}}(x_2) = \gamma_1 \mathrm{e}^{-kq_1x_2}\begin{bmatrix} 1 \\ \frac{e_{15}^\circ}{\epsilon_{11}^\circ} \end{bmatrix} + \gamma_2 \mathrm{e}^{-kq_2x_2}\begin{bmatrix} 0 \\ 1 \end{bmatrix}. \tag{3.13}$$

Then $\boldsymbol{u}$ follows from $(3.1)_1$ as: $\boldsymbol{u} = (1/\sqrt{f})\hat{\boldsymbol{u}}$, and $\boldsymbol{v}$ follows from the substitution of this latter equation into the inverse of $(2.4)_1$, which is: $\boldsymbol{v} = -\mathrm{i}f\boldsymbol{N_2}^{-1}\boldsymbol{u}'$. In the end, it is found that at the interface,

$$\begin{aligned}
&U_3(0) = \gamma_1,\\
&\varphi(0) = \frac{e_{15}^\circ}{\epsilon_{11}^\circ}\gamma_1 + \gamma_2,\\
&t_{23}(0) = \mathrm{i}k\left[\left(c_{44}^\circ + \frac{e_{15}^{\circ 2}}{\epsilon_{11}^\circ}\right)\left(q_1 + \frac{f'(0)}{2k}\right)\gamma_1 + e_{15}^\circ\left(q_2 + \frac{f'(0)}{2k}\right)\gamma_2\right],\\
&d_2(0) = -\mathrm{i}k\epsilon_{11}^\circ\left(q_2 + \frac{f'(0)}{2k}\right)\gamma_2.
\end{aligned} \tag{3.14}$$

Now the usual boundary value problems of Bleustein–Gulyaev wave propagation can be solved. For the *metalized boundary condition*, $\varphi(0) = 0$ and $t_{23}(0) = 0$. These conditions lead to a homogeneous system of two equations for the set of constants $\{\gamma_1, \gamma_2\}$. That set is non-trivial when the following *dispersion equation for the metalized boundary condition* is satisfied for $v = v_m$ (say),

$$\left(\frac{v_m}{v_T^\circ}\right)^2 = 1 + \frac{c_0}{k^2} - \left[\chi^2\left(\sqrt{1 + \frac{c_0}{k^2}} + \frac{f'(0)}{2k}\right) - \frac{f'(0)}{2k}\right]^2, \quad \chi^2 := \frac{e_{15}^{\circ 2}}{c_{44}^\circ\epsilon_{11}^\circ + e_{15}^{\circ 2}}. \tag{3.15}$$

Here, the positive quantity χ^2 is the (bulk) transverse-wave electromechanical coupling coefficient. Recall that the classic Bleustein–Gulyaev wave is non-dispersive for a *homogeneous* metalized half-space. Its speed v_m° is given by

$$\left(v_m^\circ/v_T^\circ\right)^2 = 1 - \chi^4. \tag{3.16}$$

Hence the effect of an inhomogeneity of the form found in Table 1 is readily seen from the comparison of the last two equations.

For the *free* (*un-metalized*) *boundary condition*, $t_{23}(0) = 0$ and $d_2(0) = \mathrm{i}k\epsilon_0\varphi(0)$, where ϵ_0 is the permittivity of vacuum (see for instance Royer and Dieulesaint, 2000, p. 310). These conditions lead again to a homogeneous system of two equations for the set of constants $\{\gamma_1, \gamma_2\}$. The *dispersion equation for the free boundary condition*, linking the wave speed v_f (say) to the wave number is now:

$$\left(\frac{v_f}{v_T^\circ}\right)^2 = 1 + \frac{c_0}{k^2} - \left[\chi^2 \frac{\sqrt{1 + c_0/k^2} + f'(0)/(2k)}{1 + (\epsilon_{11}^\circ/\epsilon_0)(\sqrt{1 + c_0/k^2} + f'(0)/(2k))} - \frac{f'(0)}{2k}\right]^2. \tag{3.17}$$

Comparison of v_f and v_m shows that $v_f > v_m$, whatever the choice of f in Table 1; so, by (3.11), the wave penetrates deeper into the substrate when its surface is not metalized, as is the case for a homogeneous substrate. Recall that for a homogeneous half-space, the classic Bleustein–Gulyaev wave is non-dispersive for "free" boundary conditions, and that it travels at speed v_f° given by

$$\left(v_f^\circ/v_T^\circ\right)^2 = 1 - \chi^4/\left(1 + \epsilon_{11}^\circ/\epsilon_0\right)^2. \tag{3.18}$$

Note that both v_f and v_m are such that (3.12) is verified.

In Case (ii) (profiles P0 and P6–P10), it is found that the attenuation factors are still given by (3.11), and that at the interface

$$\begin{aligned}
U_3(0) &= \left(q_1 - \frac{f'(0)}{2k}\right)\gamma_1, \\
\varphi(0) &= \frac{e_{15}^\circ}{\epsilon_{11}^\circ}\left(q_1 - \frac{f'(0)}{2k}\right)\gamma_1 + \left(q_2 - \frac{f'(0)}{2k}\right)\gamma_2, \\
t_{23}(0) &= \mathrm{i}k\left[\left(c_{44}^\circ + \frac{e_{15}^{\circ 2}}{\epsilon_{11}^\circ}\right)\left(1 - \frac{v^2}{v_T^{\circ 2}}\right)\gamma_1 + e_{15}^\circ\gamma_2\right], \\
d_2(0) &= -\mathrm{i}k\epsilon_{11}^\circ\gamma_2.
\end{aligned} \tag{3.19}$$

For the *metalized boundary condition*, the dispersion equation is now:

$$\chi^2\left(\sqrt{1 + \frac{c_0}{k^2} - \frac{v_m^2}{v_T^{\circ 2}}} - \frac{f'(0)}{2k}\right) = \left(1 - \frac{v_m^2}{v_T^{\circ 2}}\right)\left(\sqrt{1 + \frac{c_0}{k^2}} - \frac{f'(0)}{2k}\right), \tag{3.20}$$

and for the *free* (*un-metalized*) *boundary condition*, the dispersion equation is now:

$$\chi^2\left(\sqrt{1 + \frac{c_0}{k^2} - \frac{v_f^2}{v_T^{\circ 2}}} - \frac{f'(0)}{2k}\right) = \left(1 - \frac{v_f^2}{v_T^{\circ 2}}\right)\left(\sqrt{1 + \frac{c_0}{k^2}} - \frac{f'(0)}{2k} + \frac{\epsilon_{11}^\circ}{\epsilon_0}\right). \tag{3.21}$$

These equations could be rationalized but this process might introduce spurious speeds. It can be checked that they coincide respectively with (3.15) and (3.17) for the exponential inhomogeneity function P0, and with (3.16) and (3.18) for the homogeneous substrate.

3.3. Examples

Consider that the substrate is made of a functionally graded material for which the material properties at the interface $x_2 = 0$ are those of a PZT-4 ceramic (Jaffe and Berlincourt, 1965): $c_{44}^\circ = 2.56 \times 10^{10}\ \mathrm{N/m^2}$, $e_{15}^\circ = 12.7\ \mathrm{C/m^2}$, $\epsilon_{11}^\circ = 650 \times 10^{-11}\ \mathrm{F/m}$, $\rho^\circ = 7500\ \mathrm{kg/m^3}$. The permittivity of vacuum is taken as: $\epsilon_0 = 8.854 \times 10^{-12}\ \mathrm{F/m}$.

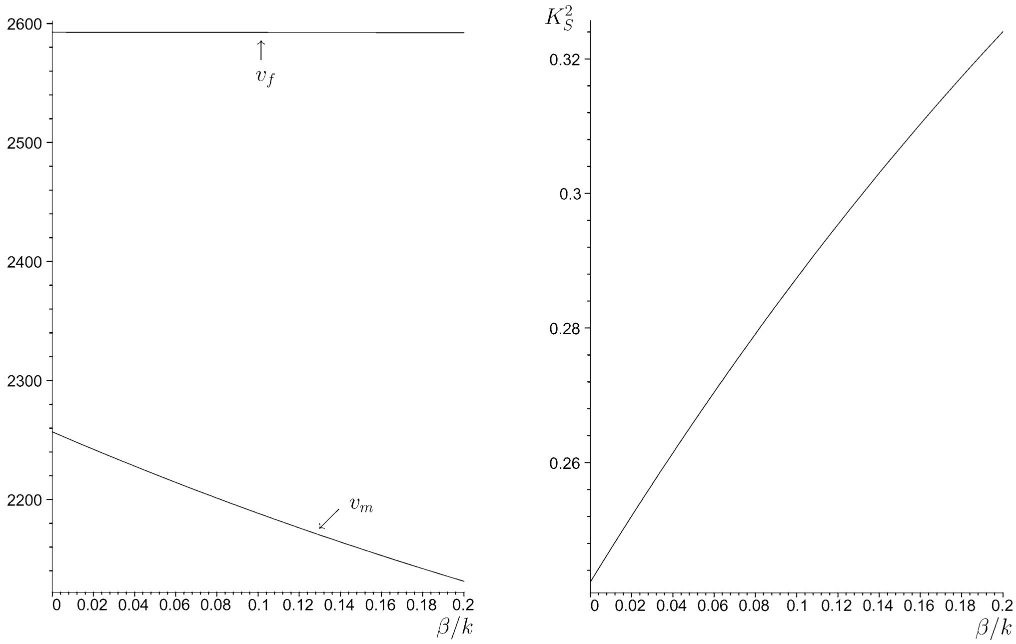

Fig. 1. Influence of a decreasing exponential inhomogeneity function on the wave speed (free and metalized boundary conditions) and on the electromechanical coupling coefficient.

When the substrate is *homogeneous*, the Bleustein–Gulyaev wave travels with speeds: $v_m^\circ = 2256.85$ m/s and $v_f^\circ = 2592.65$ m/s, for metalized and free boundary conditions, respectively. The surface *electromechanical coupling coefficient* K_S^2 is given by (Royer and Dieulesaint, 2000, p. 296),

$$K_S^2 = \frac{v_f^{\circ 2} - v_m^{\circ 2}}{v_f^{\circ 2} + (\epsilon_0/\epsilon_{11}^\circ)v_m^{\circ 2}} \approx \frac{v_f^{\circ 2} - v_m^{\circ 2}}{v_f^{\circ 2}}, \tag{3.22}$$

the latter approximation being justified in the PZT-4 case. Here, $K_S^2 \approx 0.242$.

In the first example, the inhomogeneity function is *decreasing exponential*: $f(x_2) = \exp(-2\beta x_2)$, $\beta > 0$ (profile P0 of Table 1). Then the mechanical displacement $U_3(x_2)$ varies as: $(1/\sqrt{f(x_2)})\exp -kq_1x_2 = \exp -k(q_1 - \beta/k)x_2$, and it is found here that

$$q_1 - \frac{\beta}{k} = \chi^2\left(\sqrt{1 + \frac{\beta^2}{k^2}} - \frac{\beta}{k}\right), \quad \frac{\chi^2}{\sqrt{1 + \beta^2/k^2} + \beta/k + \epsilon_{11}^\circ/\epsilon_0}, \tag{3.23}$$

for metalized and free boundary conditions, respectively. Both quantities are clearly positive and the decay is secured. The dispersion equations (3.15) and (3.17) give the wave speed in terms of the dimensionless quantity β/k. The range for this quantity is chosen so that the inhomogeneity function decreases with depth in a slower fashion than the mechanical displacement for the metalized boundary condition — for the free boundary condition, the wave speed is so close to the body wave speed ($v_f^\circ = 0.9999998 v_T$) that the displacement hardly decays at all. In other words, β/k satisfies: $2\beta/k < q_1 - \beta/k$, where the right hand-side is given by $(3.23)_1$. This is equivalent to: $\beta/k < \chi^2/(2\sqrt{1+\chi^2}) = 0.2015$. Fig. 1(a) shows the variations of v_m (lower curve) and v_f (upper curve) with β/k from 0 (homogeneous PZT-4 substrate) to 0.2. In this range, the inhomogeneity function has no noticeable influence on the speed of the Bleustein–Gulyaev wave with free boundary conditions, whereas it slows down significantly the Bleustein–Gulyaev wave with metalized boundary conditions, resulting in an increasing electromechanical coupling coefficient K_S^2 (Fig. 1(b)), from 0.242 to 0.324.

For the second example, the inhomogeneity function is *inverse quadratic*: $f(x_2) = 1/(\beta x_2 + 1)^2$, $\beta > 0$ (profile P6 of Table 1). Then the mechanical displacement $U_3(x_2)$ varies as: $(1/\sqrt{f(x_2)})\exp -kq_1x_2 = (\beta x_2 + 1)\exp -kq_1x_2$. Here the decay is secured when (3.12) is satisfied, which is equivalent to: $v < v_T$, the same condition as in the

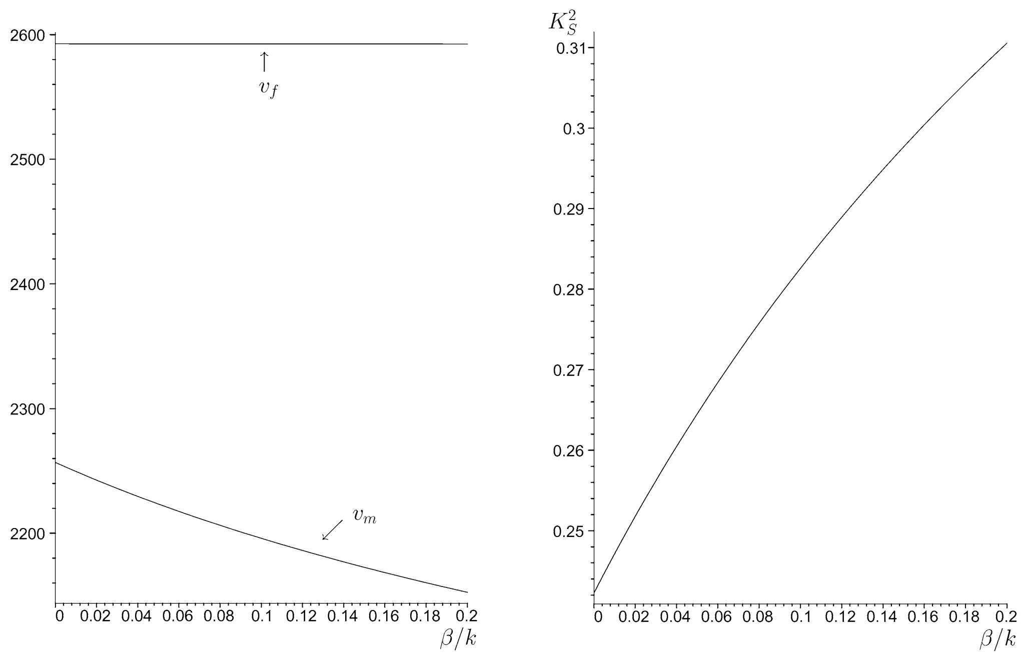

Fig. 2. Influence of an inverse quadratic inhomogeneity function on the wave speed (free and metalized boundary conditions) and on the electromechanical coupling coefficient.

homogeneous substrate. For this profile, $c_0 = 0$ and $f'(0) = -2\beta$, so that the dispersion equations (3.20) and (3.21) are easily solved. The metalized boundary condition gives:

$$\left(\frac{v_m}{v_T^\circ}\right)^2 = 1 - \frac{\chi^4}{4(1+\beta/k)^2}\left[1 + \sqrt{1 + \frac{4}{\chi^2}\left(1+\frac{\beta}{k}\right)\frac{\beta}{k}}\,\right]^2, \tag{3.24}$$

and the free boundary condition gives:

$$\left(\frac{v_f}{v_T^\circ}\right)^2 = 1 - \frac{\chi^4}{4(1+\beta/k+\epsilon_{11}^\circ/\epsilon_0)^2}\left[1 + \sqrt{1 + \frac{4}{\chi^2}\left(1+\frac{\beta}{k}+\frac{\epsilon_{11}^\circ}{\epsilon_0}\right)\frac{\beta}{k}}\,\right]^2. \tag{3.25}$$

For the purpose of comparison with the first example, Figs. 2(a) and 2(b) display the variations of the wave speeds with the dimensionless quantity β/k over the same range $0 \leqslant \beta/k \leqslant 0.2$. They show that the influence of each inhomogeneity functions is very much the same: here, the electromechanical coupling coefficient increases (from 0.242) to 0.310 instead of 0.324 for the decreasing exponential profile. The present inverse quadratic inhomogeneity is however more satisfying to consider from a "physical" point of view, because it decreases slower with depth than an exponential inhomogeneity, and it can thus describe a situation where the wave is confined near the surface while the material parameters (2.1) vanish at a greater distance.

The next section presents a third example of inhomogeneity function, this time yielding a profile for which the material parameters neither vanish nor blow-up with distance from the interface.

4. An asymptotically homogeneous half-space

Consider the well-known solution $[\boldsymbol{U}(x_2), \boldsymbol{V}(x_2)]^{\mathrm{T}}$ (say) to the piezoacoustic equations (2.4) in a *homogeneous* substrate:

$$\begin{bmatrix} \boldsymbol{U}(x_2) \\ \boldsymbol{V}(x_2) \end{bmatrix} = \gamma_1 \mathrm{e}^{-k\eta x_2} \begin{bmatrix} 1 \\ e_{15}^\circ/\epsilon_{11}^\circ \\ \mathrm{i}k\eta(c_{44}^\circ + e_{15}^{\circ 2}/\epsilon_{11}^\circ) \\ 0 \end{bmatrix} + \gamma_2 \mathrm{e}^{-kx_2} \begin{bmatrix} 0 \\ 1 \\ \mathrm{i}ke_{15}^\circ \\ -\mathrm{i}k\epsilon_{11}^\circ \end{bmatrix}, \quad \eta := \sqrt{1 - \left(\frac{v}{v_T^\circ}\right)^2}. \tag{4.1}$$

These functions satisfy (2.4) when $f \equiv 1$ that is,

$$\boldsymbol{U}' = \mathrm{i}\boldsymbol{N_2}\boldsymbol{V}, \qquad \boldsymbol{V}' = \mathrm{i}k^2\boldsymbol{K}\boldsymbol{U}. \tag{4.2}$$

Now seek a solution $[\boldsymbol{u}, \boldsymbol{v}]^{\mathrm{T}}$ to the piezoacoustic equations (2.4) for the functionally graded material in the form:

$$\boldsymbol{u} = \frac{u_0}{k}\boldsymbol{U}' + u_1\boldsymbol{U}, \qquad \boldsymbol{v} = \frac{v_0}{k}\boldsymbol{V}' + v_1\boldsymbol{V}, \tag{4.3}$$

where u_0, u_1, v_0, v_1 are yet unknown scalar functions of x_2. By differentiation and substitution, it is found that if they satisfy

$$u_0 = v_0/f, \quad u_0'/k + u_1 = v_1/f, \quad v_0'/k + v_1 = f u_1, \quad u_1' = 0, \quad v_1' = 0, \tag{4.4}$$

then (2.4) is satisfied. The choice

$$u_0 = 1/\sqrt{f}, \quad v_0 = \sqrt{f}, \quad u_1 = -\frac{\beta}{k}\tanh\delta, \quad v_1 = -\frac{\beta}{k\tanh\delta}, \tag{4.5}$$

(where β, δ are constants) takes care of $(4.4)_{1,4,5}$. Then $(4.4)_{2,3}$ both reduce to

$$\left(\sqrt{f}\right)' - (\beta/\tanh\delta) = -(\beta\tanh\delta) f, \tag{4.6}$$

a solution of which is

$$f(x_2) = \frac{\tanh^2(\beta x_2 + \delta)}{\tanh^2\delta}. \tag{4.7}$$

This inhomogeneity function has the sought-after property of never vanishing (if $\delta > 0$) nor blowing-up as x_2 spans the whole half-space occupied by the substrate. It describes a material for which the parameters $c_{44}(x_2)$, $e_{15}(x_2)$, $\epsilon_{11}(x_2)$, $\rho(x_2)$ change smoothly from their initial values c_{44}°, e_{15}°, ϵ_{11}°, ρ° at the interface $x_2 = 0$ to a higher asymptotic value $\{c_{44}^\circ, e_{15}^\circ, \epsilon_{11}^\circ, \rho^\circ\}/\tanh^2\delta$, where $\delta > 0$ is an adjustable parameter. The parameter β can also be adjusted to describe a not only a slow but also a rapid variation with depth, which would confine the inhomogeneity to a thin layer near the surface. This latter opportunity was excluded with the profiles of Section 3, because of their blow-up or vanishing behaviors.

Now the substitution of f into (4.5) and then into the solution (4.3), leads to the following expressions for the fields at the interface,

$$\begin{aligned}
U_3(0) &= \left(\eta + \frac{\beta}{k}\tanh\delta\right)\gamma_1,\\
\varphi(0) &= \frac{e_{15}^\circ}{\epsilon_{11}^\circ}\left(\eta + \frac{\beta}{k}\tanh\delta\right)\gamma_1 + \left(1 + \frac{\beta}{k}\tanh\delta\right)\gamma_2,\\
t_{23}(0) &= \mathrm{i}k\left[\left(c_{44}^\circ + \frac{e_{15}^{\circ 2}}{\epsilon_{11}^\circ}\right)\eta\left(\eta + \frac{\beta}{k\tanh\delta}\right)\gamma_1 + e_{15}^\circ\left(1 + \frac{\beta}{k\tanh\delta}\right)\gamma_2\right],\\
d_2(0) &= -\mathrm{i}k\epsilon_{11}^\circ\left(1 + \frac{\beta}{k\tanh\delta}\right)\gamma_2.
\end{aligned} \tag{4.8}$$

The *dispersion equation for the metalized boundary condition* is a quadratic in $\eta = \sqrt{1 - (v_m/v_T{}^\circ)^2}$:

$$\eta\left(\eta + \frac{\beta}{k\tanh\delta}\right)\left(1 + \frac{\beta}{k}\tanh\delta\right) - \chi^2\left(\eta + \frac{\beta}{k}\tanh\delta\right)\left(1 + \frac{\beta}{k\tanh\delta}\right) = 0. \tag{4.9}$$

At $\beta = 0$, the function f in (4.7) is that of a homogeneous substrate ($f \equiv 1$), and this equation gives: $\eta = \chi^2$, which, once squared, is (3.16).

The *dispersion equation for the free boundary condition* is also a quadratic, now in $\eta = \sqrt{1 - (v_f/v_T^\circ)^2}$:

$$\eta\left(\eta + \frac{\beta}{k\tanh\delta}\right)\left[\frac{1 + (\beta/k)\tanh\delta}{1 + \beta/(k\tanh\delta)} + \frac{\epsilon_{11}^\circ}{\epsilon_0}\right] - \chi^2\left(\eta + \frac{\beta}{k}\tanh\delta\right) = 0. \tag{4.10}$$

At $\beta = 0$, this equation gives: $\eta(1 + \epsilon_{11}^\circ/\epsilon_0) = \chi^2$, which, once squared, is (3.18).

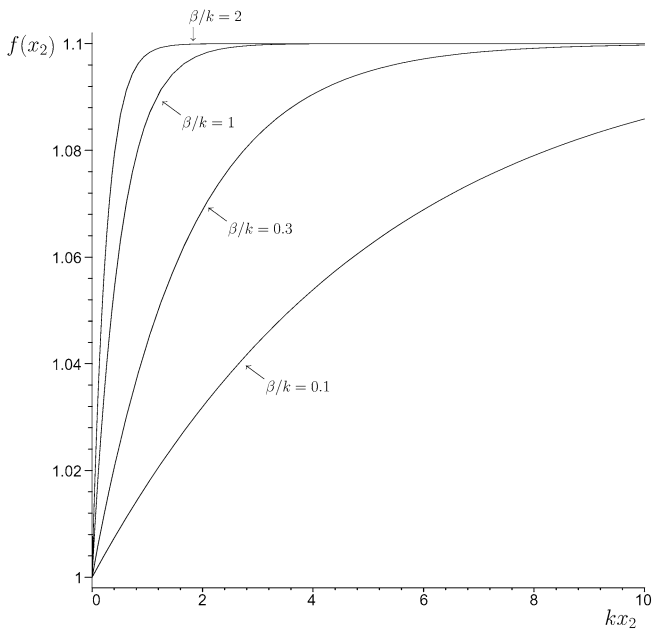

Fig. 3. Variation of an asymptotically homogeneous profile with depth for four different values of the dispersion parameter β/k.

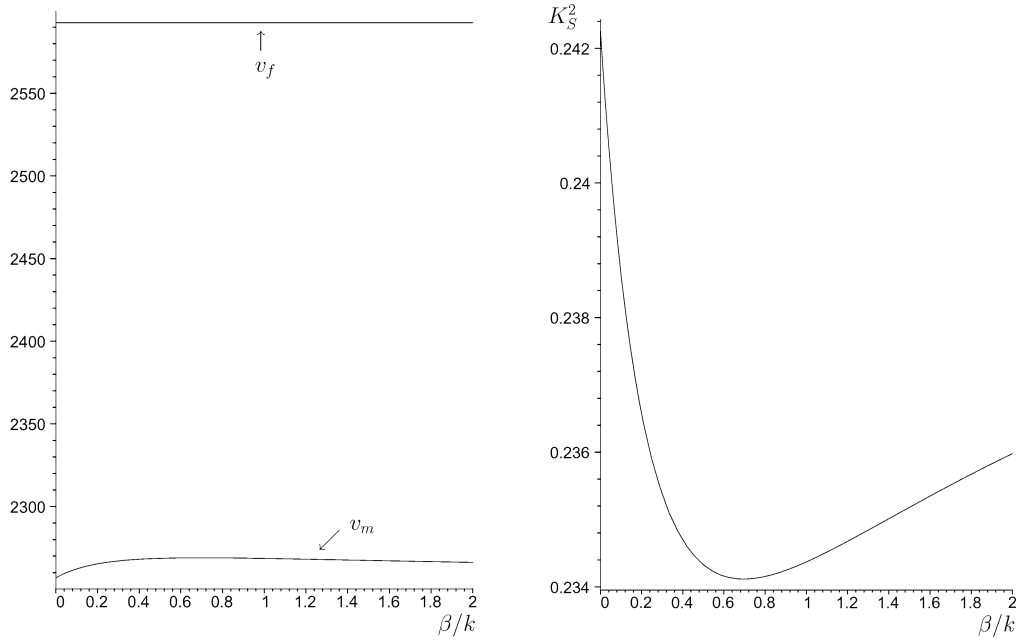

Fig. 4. Influence of an asymptotically homogeneous profile on the wave speed (free and metalized boundary conditions) and on the electromechanical coupling coefficient.

Each dispersion equation is a quadratic giving a priori two roots: one tends to $\eta = 0$ (and so $v = v_T$) as $\beta \to 0$ (homogeneous substrate) and can be ruled out.

For the third example, consider an inhomogeneous substrate whose properties increase continuously according to (4.7) from those of a PZT-4 ceramic at the interface $x_2 = 0$ to asymptotic values which are 10% greater ($\tanh\delta = 1/\sqrt{1.1} \approx 0.953$). Fig. 3 shows the variations of the inhomogeneity function with depth, for several values of the parameter β/k: clearly for $\beta/k > 2$, the inhomogeneity is confined within a layer near the surface whose thickness is less than a wavelength. Fig. 4(a) shows the variations of v_m (lower curve) and v_f (upper curve) with β/k from 0 (homogeneous PZT-4 substrate) to 2. In this range, the inhomogeneity function again has no noticeable influence on the speed of the Bleustein–Gulyaev wave with free boundary conditions. However here the speed of the Bleustein–Gulyaev wave with metalized boundary conditions is *always greater* than in the homogeneous substrate, resulting in a smaller electromechanical coupling coefficient K_S^2 (Fig. 4(b)).

5. More inhomogeneity functions

The previous section presented a method to derive an inhomogeneity function for which exact Bleustein–Gulyaev solutions are possible, but which did not rely on finding governing equations with constant coefficients as in Section 3. That method is due in essence to Varley and Seymour (1988) (see also Erdogan and Ozturk, 1992) and it can be generalized to yield an infinity of such inhomogeneity functions.

First, seek a solution $[\boldsymbol{u}, \boldsymbol{v}]^{\mathrm{T}}$ to the piezoacoustic equations (2.4) in the form:

$$\boldsymbol{u} = \sum_{n=0}^{p} \frac{u_n}{k^{p-n}} \boldsymbol{U}^{(p-n)}, \qquad \boldsymbol{v} = \sum_{n=0}^{p} \frac{v_n}{k^{p-n}} \boldsymbol{V}^{(p-n)}, \tag{5.1}$$

(thus (4.3) corresponds to $p = 1$), where u_n, v_n $(n = 0, \dots, p)$ are unknown functions of x_2. Differentiate once, substitute into (2.4), and use (4.2) to get

$$\frac{1}{k^p}\left(u_0 - \frac{1}{f}v_0\right)\boldsymbol{U}^{(p-1)} + \sum_{n=1}^{p} \frac{1}{k^{p-n}}\left(\frac{u'_{n-1}}{k} + u_n - \frac{1}{f}v_n\right)\boldsymbol{U}^{(p-n-1)} + u'_p\boldsymbol{U} = \boldsymbol{0}, \tag{5.2}$$

and

$$\frac{1}{k^p}(v_0 - f u_0)\boldsymbol{V}^{(p-1)} + \sum_{n=1}^{p} \frac{1}{k^{p-n}}\left(\frac{v'_{n-1}}{k} + v_n - f u_n\right)\boldsymbol{V}^{(p-n-1)} + v'_p\boldsymbol{V} = \boldsymbol{0}. \tag{5.3}$$

Both differential equations are satisfied when the following set of equations is satisfied,

$$\begin{aligned} &u_0 = 1/\sqrt{f}, \quad v_0 = \sqrt{f}, \quad u'_p = 0, \quad v'_p = 0, \\ &u'_{n-1}/k + u_n = v_n/f, \qquad v'_{n-1}/k + v_n = f u_n. \end{aligned} \tag{5.4}$$

Varley and Seymour (1988) found an infinity of f such that this set can be completely solved. Because there is little value in reproducing their derivations, the reader is referred to their article for explicit examples. It suffices to notice that in general the solutions are combinations of trigonometric and/or hyperbolic functions, and that a great number of arbitrary constants are at disposal for curve fitting. For instance at $p = 2$, Varley and Seymour present at least 16 possible forms for f, each involving 5 arbitrary constants. As another example, it can be checked directly here that the polynomial function

$$f(x_2) = (\beta x_2 + 1)^{2p}, \tag{5.5}$$

where p is an integer, is also suitable; then,

$$u_n = b_n(\beta x_2 + 1)^{-(p+n)}, \quad v_n = a_n(\beta x_2 + 1)^{p-n} \quad (n = 0, \dots, p), \tag{5.6}$$

where a_n and b_n are determined by recurrence from $a_0 = b_0 = 1$ and

$$a_n = -\frac{\beta}{2kn}(p - n + 1)(p + n)a_{n-1}, \quad b_n = \frac{p - n}{p + n}a_n \quad (n = 1, \dots, p). \tag{5.7}$$

References

Azis, M.I., Clements, D.L., 2001. A boundary element method for anisotropic inhomogeneous elasticity. Int. J. Solids Struct. 38, 574–5763.
Bhattacharya, S.N., 1970. Exact solutions of SH wave equation for inhomogeneous media. Bul. Seism. Soc. Am. 60, 1847–1859.
Bleustein, J.L., 1968. A new surface wave in piezoelectric materials. Appl. Phys. Lett. 13, 412–413.
Chen, J., Liu, Z., 2005a. Transient response of a mode III crack in an orthotropic functionally graded strip. Eur. J. Mech. A Solids 24, 325–336.

Chen, J., Liu, Z., 2005b. On the dynamic behavior of a functionally graded piezoelectric strip with periodic cracks vertical to the boundary. Int. J. Solids Struct. 42, 3133–3146.

Chen, J., Soh, A.K., Liu, J., Liu, Z.X., 2004. Transient anti-plane crack problem of a functionally graded piezoelectric strip bonded to elastic layers. Acta Mech. 169, 87–100.

Cohen, H., Wang, C.-C., 1992. Some equilibrium problems for compressible, anisotropic, laminated nonlinearly elastic bodies. Arch. Rational Mech. Anal. 119, 1–34.

Deresiewicz, H., 1962. A note on Love waves in a homogeneous crust overlying an inhomogeneous stratum. Bul. Seism. Soc. Am. 52, 639–645.

Destrade, M., 2001. The explicit secular equation for surface acoustic waves in monoclinic elastic crystals. J. Acoust. Soc. Am. 109, 1398–1402.

Dutta, S., 1963. Love waves in a non-homogeneous internal stratum lying between two semi-infinite isotropic media. Geophys. 28, 156–160.

Erdogan, F., Ozturk, M., 1992. Diffusion problems in bonded nonhomogeneous materials with an interface cut. Int. J. Engrg. Sci. 30, 1507–1523. Geophys. 28, 156–160.

Feng, W.J., Su, R.K.L., 2006. Dynamic internal crack problem of a functionally graded magneto-electro-elastic strip. Int. J. Solids Struct., in press.

Gubernatis, J.E., Maradudin, A.A., 1987. A Laguerre series approach to the calculation of wave properties for surfaces of inhomogeneous elastic materials. Wave Motion 9, 111–121.

Gulyaev, Yu.V., 1969. Electroacoustic surface waves in piezoelectric materials. JETP Lett. 9, 37–38.

Guo, L.-C., Wu, L.-Z., Zeng, T., 2005a. The dynamic response of an edge crack in a functionally graded orthotropic strip. Mech. Res. Comm. 32, 385–400.

Guo, L.-C., Wu, L.-Z., Zeng, T., Cao, D.H., 2005b. The transient response of a coating-substrate structure with a crack in the functionally graded interfacial layer. Comp. Struct. 70, 109–119.

Hasanyan, D.J., Piliposian, G.T., Kamalyan, A.H., Karakhanyan, M.I., 2003. Some dynamic problems for elastic materials with functional inhomogeneities: anti-plane deformations. Continuum Mech. Thermodyn. 15, 519–527.

Jaffe, H., Berlincourt, D.A., 1965. Piezoelectric transducer materials. Proc. IEEE 53, 1372–1386.

Jin, B., Soh, A.K., Zhong, Z., 2003. Propagation of an anti-plane moving crack in a functionally graded piezoelectric strip. Arch. Appl. Mech. 73, 252–260.

Kadota, M., Yoneda, T., Fujimoto, K., Nakao, T., Takata, E., 2001. Very small-sized resonator IF filter using shear horizontal wave on quartz substrate. IEEE Ultrason. Symp. Proc. 1, 65–68.

Kwon, S.M., 2004. On the dynamic propagation of an anti-plane shear crack in a functionally graded piezoelectric strip. Acta Mech. 167, 73–89.

Kwon, S.M., Lee, K.Y., 2003. An anti-plane propagating crack in a functionally graded piezoelectric strip bonded to a homogeneous piezoelectric strip. Arch. Appl. Mech. 73, 348–366.

Lakhtakia, A., 1994. Axial propagation in piezoelectric, continuously twisted, structurally chiral mediums. J. Acoust. Soc. Am. 95, 2961.

Lefebvre, J.E., Zhang, V., Gazalet, J., Gryba, T., Sadaune, V., 2001. Acoustic wave propagation in continuous functionally graded plates: an extension of the Legendre polynomial approach. IEEE Trans. Ultras. Ferr. Freq. Control 48, 1332–1339.

Liu, G.R., Tani, J., 1994. Surface waves in functionally gradient piezoelectric plates. ASME J. Vib. Acoust. 116, 440–448.

Liu, J., Wang, Z.K., 2005. The propagation behavior of Love waves in a functionally graded layered piezoelectric structure. Smart Mat. Struct. 14, 137–146.

Ma, L., Wu, L.-Z., Zhou, Z.-G., Guo, L.-C., Shi, L.-P., 2004. Scattering of harmonic anti-plane shear waves by two collinear cracks in functionally graded piezoelectric materials. Eur. J. Mech. A Solids 23, 633–643.

Ma, L., Wu, L.-Z., Zhou, Z.-G., Guo, L.-C., 2005a. Scattering of the harmonic anti-plane shear waves by a crack in functionally graded piezoelectric materials. Comp. Struct. 69, 436–441.

Ma, L., Wu, L.-Z., Guo, L.-C., Zhou, Z.-G., 2005b. On the moving Griffith crack in a non-homogeneous orthotropic medium. Eur. J. Mech. A Solids 24, 393–405.

Maugin, G.A., 1983. Elastic surface waves with transverse horizontal polarization. Adv. Appl. Mech. 23, 373–434.

Pan, E., Han, F., 2005. Exact solution for functionally graded and layered magneto-electro-elastic plates. Int. J. Engrg. Sci. 43, 321–339.

Royer, D., Dieulesaint, E., 2000. Elastic Waves in Solids I. Free and Guided Propagation. Springer, Berlin.

Saccomandi, G., 1999. On inhomogeneous deformations in finite thermoelasticity. IMA J. Appl. Math. 63, 131–148.

Sladek, J., Sladek, V., Zhang, C.Z., 2005. A meshless local boundary integral equation method for dynamic anti-plane shear crack problem in functionally graded materials. Eng. Analysis Bound. Elements 29, 334–342.

Sun, J.-L., Zhou, Z.-G., Wang, B., 2005. Dynamic behavior of a crack in a functionally graded piezoelectric strip bonded to two dissimilar half piezoelectric material planes. Acta Mech. 176, 45–60.

Varley, E., Seymour, B., 1988. A method for obtaining exact solutions to partial differential equations with variable coefficients. Stud. Appl. Math. 78, 183–225.

Viktorov, I.A., 1979. Types of acoustic surface waves in solids (review). Sov. Phys. Acoust. 25, 1–9.

Wang, B.L., 2003. A mode III crack in functionally graded piezoelectric materials. Mech. Res. Comm. 30, 151–159.

Wilson, J.T., 1942. Surface waves in a heterogeneous medium. Bul. Seism. Soc. Am. 32, 297–304.